Gray Balance Control Loop for Digital Color Printing Systems

Lalit K. Mestha, R. Enrique Viturro, and Yao Rong Wang, Xerox Corporation, Wilson Center for Research and Technology, Webster, New York, USA; Sohail A. Dianat, Professor of Electrical Engineering, Rochester Institute of Technology. Rochester, New York, USA

Abstract

Four-color process printers generally use gray balance for achieving color balance. Here we describe a novel gray balance control system which uses multivariable state feedback principles. We show that the system performance is greatly improved and the requirements on number of color measurements per calibration initialization are greatly reduced. A synthesis of a state space control model, feedback controller and TRC smoothing techniques are discussed in detail to achieve good prints after gray balance. Experimental results are shown to validate the approach when used for real-time feedback control of color systems.

Introduction

Companies involved in the development of digital color print engines are continuously looking for ways to improve the total image quality over time. The output of marking devices drift over time (or deviate from predetermined optimum standards) due to variety of factors. These factors include environmental conditions (temperature, relative humidity, etc.), use patterns, the type of media, variations in media, variations from original models used in initialization, general wear, etc. When a marking device is originally initialized, and, thereafter, re-initialized at regular or irregular intervals, it is calibrated and characterized to produce outputs as close as possible to a reference standard.[1] The full calibration and characterization process is time consuming and expensive, particularly because specific expertise is required to enable them. Four-color process printers generally use gray balance as a starting point for achieving color balance and linearization to a selected color axis, because it is easy to implement in practice.

Gray balance is the procedure used by print operators to accurately reproduce a neutral gray image when the image is printed with cyan, magenta, and yellow halftone dots. A midtone three-color gray can be comprised of 50% yellow, 50% Magenta and 50% Cyan. When the gray balance procedure is implemented, the printer will render a near neutral gray tone with these separations, which can be set to give a particular tone level whose color value can be tuned to have the desired reference value (e.g., L*=50, a*=0, b*=0 for neutral gray). Individual color values are tuned between 0 to 100% with the gray balance procedure to produce the desired tone color, so that the printer will faithfully give pleasing color for all other combinations of CMY.

If the gray balance reference is altered, then the color balance will also be altered. In system terms, the outcome of the gray balance procedure can be thought of as a method to generate inverse maps to linearize the printer so that when used, the printer will be steered to follow a desired reference. For example, when the reference values are selected on the neutral axis, the printer with a gray balanced inverse map will be linear to neutral colors, but is not linear for other regions of the color axes in the three dimensional color space. If the reference values are off-neutral, then it is steered to follow the off-neutral axis, effectively making the printer linear to the off-neutral reference axis.

Our goal in this paper is to show how to construct an efficient set of gray balance TRCs using control methodologies since these approaches can greatly reduce the number of measurements required for regular updates to overcome color drift.

Gray Balance for Digital Printers

Normally, the calibration and characterization of a conventional four-color (cyan, magenta, yellow and black) printer or copier involves at least the following processes[2]: (1) generating a 3D look-up table (LUT) for mapping device independent parameter space to CMY space; (2) executing a GCR (gray component replacement)/UCR (under color removal) strategy to convert the CMY space parameters to CMYK space parameters which represent the colors of a typical four-color marking device; (3) constructing marking device TRCs to account for marking device variability (normally done at the time of manufacturing or whenever the printer calibration and characterization process is involved); and (4) applying a suitable half-toning strategy to convert the CMYK continuous tone description obtained after using the 3D LUTs in steps 1 and 2 above and 1D LUTs in step 3 above, to the image, to a binary description (e.g., bits to be received by a raster output scanner or similar device for outputting the image). The first two steps generally use printer characterization to develop the LUTs. The third step is normally called calibration, which is the subject of this document.

Control Based Methodologies for Gray Balancing Digital Printers

In the closed loop color calibration system, sensor measures the response of the output (in here, the L*a*b* values of printed color patches). Sensor values are then compared to the desired response (that is the reference L*a*b* values). The difference in these values are then used to create new CMYK values so that when the patches are printed next time using the most current CMYK values the difference in the desired response to the measured response is near zero. The printing, measuring, comparing and the generation of CMYK process are repeated until satisfactory results are obtained. With this kind of successive iterations, we achieve the new CMYK values to produce the desired response (the reference). The printer inverse map for the desired reference L*a*b* values is now the new CMYK values obtained after reaching the desired reference, i.e., when the error between the reference L*a*b* values to the measured L*a*b* values is equal to or near zero. The gray balance map is obtained when the desired reference values are set to neutral gray or off-neutral gray depending on the type of gray balance is required; e.g., SWOP gray, Neutral gray etc.

There are at least three major problems involved in developing this kind of gray balance procedure. The first problem is with the non-invertibility nature of the four-color printer when the black separation is included in this loop. Secondly, the iteration procedure has to converge fast, say in one or two steps otherwise, customers may waste media (paper) while performing gray balance. The third problem is associated with the boundary colors; i.e., colors near the highlights and shadow regions of the neutral color axes. Using combinations of controls and processing algorithms in multidimensional color space, we have overcome these problems.

To overcome the non-invertibility problem due to the addition of black separation, we linearize the gray axis by performing the gray balance procedure on CMY separations. Linearization of black separation is performed along L* axis by treating it separately. While performing iterations to find the inverse map for CMY gray, we use CMY values as control actuators. That means, for an open-loop system, the input values are CMY and the output values are L*a*b* and the sensor or the sensing sub-system associated with the sensor is considered as part of the overall system model. The input-output diagram for a single color CMY gray balance is shown schematically in Fig. 2.

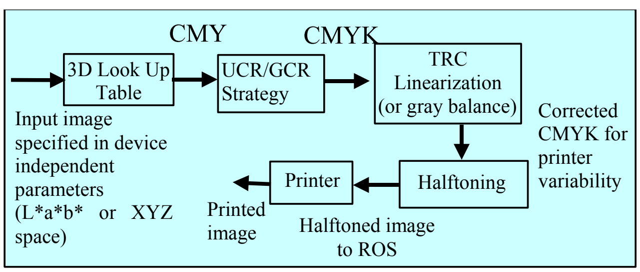

*Figure 1. Schematic diagram of an image path with input image pixels to printed image pixels shown in L*a*b**

The vector $\underline{V}$ represents small deviations in C, M, Y, which is used during iterations. Measured L*a*b* values are shown by the vector $\underline{X}$. Nominal CMY values are obtained from one of the following two methods – using printer inverse model or simply through assignment based on the desired reference L*a*b* values. In this diagram we show an example for C=M=Y=50%, as the nominal values for an equivalent neutral gray reference L*=50, a*=0 and b*=0. The nominal value could be simply the best CMY values obtained from the previous iterations also. For example, when the control algorithm is used for gray balancing the print engine, a simple assignment rule is found sufficient (i.e., nominal CMY values are chosen using C=M=Y=L*). If the printer map is constructed using Neugebauer or other models, which is often readily available in the Color Rendition Dictionary, then the nominal CMY values are calculated for each of the reference L*a*b* values.

Once the nominal values are chosen, now the problem of finding the correct CMY values is to search for the best $\underline{V}$ vector iteratively by printing, measuring L*a*b* values and comparing to the reference L*a*b* values for selected patches along the reference axis. We need an appropriate error-processing algorithm so that the iterations converge and many of the closed loop performance criteria of the iterative loop (i.e., faster convergence time – use of one to two iterations, zero/minimal steady-state errors, no transient response, low sensitivity to changes in system, large stability bounds etc.,) are met. The design of error-processing algorithm requires theoretical knowledge of Multi-Input Multi-Output (MIMO) control.[4]

Considering the printer input-output characteristic as linear (which is generally true at the nominal CMY values, see Fig. 3), we first develop a state model for the open loop system of Fig. 2. After that, we present the design of state feedback for the iterative gray balance loop.

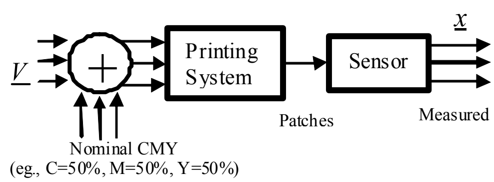

Figure 2. Diagram representing open loop system for CMY primary printing system

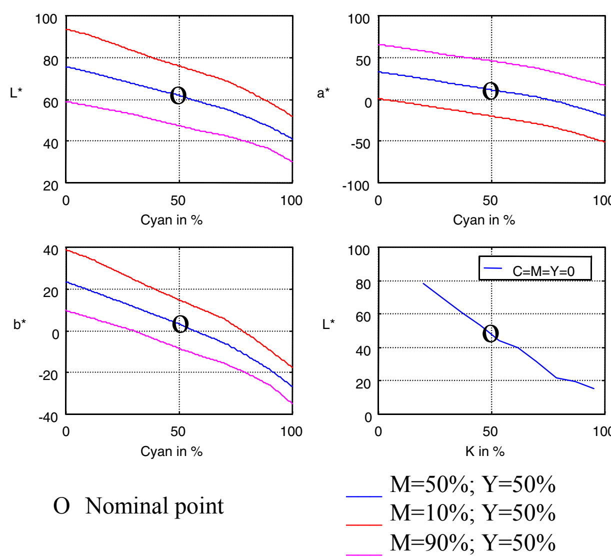

*Figure 3. Diagram representing L*a*b* values when C is varied at constant M& Y.*

At the nominal CMY inputs, we can approximately represent the dynamical behavior of the single color reproduction system using the first order finite difference (discrete) equation with dependence on the print number. If k is the print number (more appropriately called iteration number), the open loop system equation for a single color is written in terms of the printer Jacobian – the first derivative between the output and the input values -- which is given by:

$$\underline{x}(k+1) = \underline{B}\underline{V}(k) + \underline{x}_o$$

$$Where\ , \quad \underline{x} = \begin{bmatrix} L^* \\ a^* \\ b^* \end{bmatrix}, \quad \underline{V} = \begin{bmatrix} \delta C \\ \delta M \\ \delta Y \end{bmatrix}, \quad \underline{B} = \begin{bmatrix} \frac{\partial L^*}{\partial C} & \frac{\partial L^*}{\partial M} & \frac{\partial L^*}{\partial Y} \\ \frac{\partial a^*}{\partial C} & \frac{\partial a^*}{\partial M} & \frac{\partial a^*}{\partial Y} \\ \frac{\partial b^*}{\partial C} & \frac{\partial b^*}{\partial M} & \frac{\partial b^*}{\partial Y} \end{bmatrix}$$

$$\underline{x}_o = \begin{bmatrix} L^* \\ a^* \\ b^* \end{bmatrix} \text{values for nominal CMY}. \tag{1}$$

When the open loop system of Fig. 2 is closed with a gain matrix and an integrator as error-processing controller (see Fig. 4 below), the closed loop state-space model is obtained by modeling the controller as follows. Here, the multivariable gain and the integrator becomes the compensator for the iterative loop.

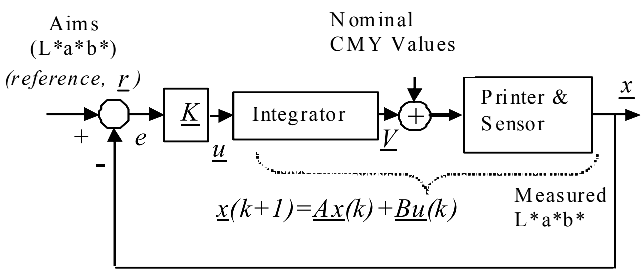

Figure 4. Closed loop with a gain and the integrator as the error-processing controller

The input to the integrator is denoted by the vector $\underline{u}(k)$. Using this formulation, the integrator can be modeled as follows.

$$\underline{V}(k) = \underline{V}(k-1) + \underline{u}(k) \tag{2}$$

Substituting Eq. 2 into Eq. 1 for $k+1^{th}$ iteration, the open loop equation becomes,

$$\underline{x}(k+1) = \underline{B}[\underline{V}(k-1) + \underline{u}(k)] + \underline{x}_0 \tag{3}$$

Now, we go through some algebraic simplification to derive an augmented open loop state equation with an explicitly introduced integrator. Consider the representation of Eq. 1 for the k^{th} print, which is shown below.

$$\underline{x}(k) = \underline{B}\underline{V}(k-1) + \underline{x}_0 \tag{4}$$

It is important to note couple of assumptions here. The Jacobian matrix of the printer is assumed time–invariant. System remains linear and $\underline{x}_0$ comprising of L*, a*, b* vector for nominal CMY values is also time invariant. There may be some error in this kind of assumption depending on how much the printer drifts during the lapse time between iterations. This type of modeling error becomes insignificant since modeling uncertainties of the type described above contribute very little to the output color.

If the Jacobian matrix is invertible, which is not always true at gamut boundaries, Eq. 4 can be written as follows

$$\underline{V}(k-1) = \underline{B}^{-1}\underline{x}(k) - \underline{B}^{-1}\underline{x}_0 \tag{5}$$

Invertibility of the Jacobian matrix leads to full rank, which turns out as an important condition/requirement for designing the gain matrix. Since the matrix is 3x3 for any given color and contains 9 elements, some those elements could be zeros and hence is still invertible. For example, change in input cyan can make L* invariant, but a* and b* could still vary. If none of L*, a* and b* change with respect to change in input cyan, then cyan is not an actuator for controlling the output, which is normally the case at the boundary (i.e., at C=0 and/or C=100%). Under those circumstances, an order reduction in the control loop is required. Substituting Eq. 5 in Eq. 4 we can obtain a state space representation.

$$\underline{x}(k+1) = \underline{B}[\underline{B}^{-1}\underline{x}(k) - \underline{B}^{-1}\underline{x}_0 + \underline{u}(k)] + \underline{x}_0 \tag{6}$$

Further reducing Eq. 6 leads to the standard state variable form described in text books[4]

$$\begin{aligned} \underline{x}(k+1) &= \underline{A}\underline{x}(k) + \underline{B}\underline{u}(k) \\ \underline{y}(k) &= \underline{C}\underline{x}(k) \end{aligned} \tag{7}$$

where the matrix $\underline{A} = \underline{I}_{3x3}$, the identity matrix which carries the meaning of a system matrix, $\underline{C} = \underline{I}_{3x3}$ the output matrix, and the output equation in Eq. 7 is same as the states. Clearly, the output values for nominal CMY inputs are cancelled in the final state equation. If the printer drifted during the time between calibration prints, then $\underline{x}_0$ will not be cancelled. On the other hand, for the purpose of controls, we can still lump those quantities as uncertainties in the model, because the first approximation has captured most of the major system dynamics.

It is important to note here that the model described by Eq. 7 is applicable to controlling a single desired color. The Jacobian matrix is different for different colors and may not differ much between printers because, on the whole, in printing systems the gradient of output colors with respect to their primaries behave in an orderly way.

Gray Balance TRCs Using State Feedback

In this section we show how a first order state space model shown above can be used for constructing CMY TRCs. The iterative procedure described above for single color is extended for multiple points along the neutral axis for input digital values between 0 – 255 to obtain a complete TRC function for each of the CMY separations. In the example shown in Table 1, we have chosen ten reference values along the neutral axis to perform neutral gray balance with CMY. In this particular example, L* values are selected between 0-100 and a* and b* values are set equal to zero. Since each colors are independently controlled to find the best CMY iteratively, we call them control nodes.

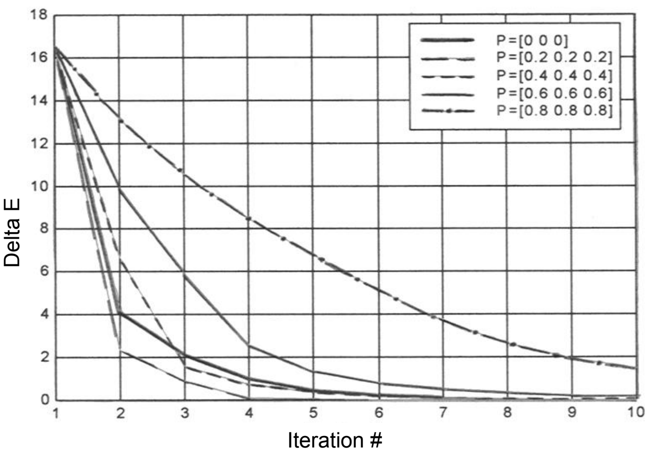

Figure 5. Convergence of norm of error vector for single gray color with repeat iteration numbers

The error between the measured L*a*b* values and the corresponding target reference colors is multiplied by the gain matrix, $\underline{K}$, to produce a small correction to the nominal CMY values. The gain matrix is designed using MIMO pole placement or MIMO Optimal Control methods described in Reference 4. The integrator integrates the weighted error between the desired L*a*b* values to the measured L*a*b* values corresponding to each of the control nodes. Accordingly from Fig. 4, the control vector can be written as:

$$\underline{u}(k)=\underline{K}\underline{e}(k) \tag{8}$$

The convergence plot of the norm of the error vector $e(k)$, which is also called ΔE, for a single color with respect to multiple iteration numbers is shown in Fig. 5 for various pole locations. Table 1 shows the output digital values for the control patches, which are obtained after convergence to the target values. Iterations can occur until the detected differences between the target values and actual output values are less than a predetermined value. After reaching the accuracy, iterations are stopped. Sometimes CMY values from last successive iterations (also called 'best actuators') depending on the type of algorithms can be used while constructing the TRCs. Iteration numbers can be adjusted by using proper values of poles. For pole locations [0,0,0], satisfactory ΔE can be reached in one iteration, if the print engine has not drifted too far away from the nominal linear state. In our example, we were able to reach convergence in one iteration for a print engine drift of ΔE=6 or so. Also, it can be shown that, for pole locations [0,0,0], the gain matrix, $\underline{K}$, is equal to the inverse of the Jacobian matrix, $\underline{B}$. CMY-TRCs are then constructed from the best CMY values by mapping the reference colors with corresponding controlled CMY values (i.e., by mapping L*, a*, b* to CMY). In particular when neutral gray colors are used as reference colors, as in Table 1, input L* is mapped to input CMY values on the TRC curves. Black TRC is constructed by first finding the best gain values for the black separation by applying similar state feedback control law shown in Eq. 8. Here, we use single gain value at each control point when compared to 9 gain values as in CMY process gray. Gain values are calculated using input-output sensivity data and poleplacement algorithm for black separation. Uncontrolled points that are in between the control points are constructed using TRC smoothing algorithm.

Table 1: Reference Values and Input-Output CMY Map Obtained After Using State Feedback Controller

Reference values			Input digital values (100-L*)*2.55			Output digital values (after control)		
L*	a*	b*	Cyan	Magenta	Yellow	Cyan	Magenta	Yellow
90.00	0	0	25.5	25.5	25.5	14.78	8.85	28.42
83.89	0	0	41.08	41.08	41.08	27.25	21.79	40.28
77.78	0	0	56.67	56.67	56.67	38.56	37.42	55.04
71.67	0	0	72.25	72.25	72.25	57.21	55.46	69.68
65.56	0	0	87.83	87.83	87.83	73.85	70.05	88.62
59.44	0	0	103.42	103.42	103.42	89.56	84.78	105.55
53.33	0	0	119.00	119.00	119.00	117.61	106.24	121.93
47.22	0	0	134.58	134.58	134.58	139.37	130.31	141.06
41.11	0	0	150.17	150.17	150.17	166.96	156.90	163.63
35.00	0	0	165.75	165.75	165.75	187.60	185.46	190.93

TRC Smoothing Algorithm

To obtain a smooth TRC by joining all the control nodes, one can think of using linear or cubic spline interpolation algorithms, which blindly interpolates the data points. Smooth functions are desirable to remove other image artifacts, such as contours due to gray level jumps. This type of interpolation will not give smooth function. Hence, we developed a new smoothing algorithm based on reaching trade-offs between good agreement with data and smoothness of the curve. The theory behind the algorithm is described in Reference 5 and will be published elsewhere.

Figure 6 below shows the CMYK TRCs with control points when the reference values of the control nodes are set to neutral (i.e., a*=0, b*=0). The region close to the origin represents the highlight area and the region close to the [255,255] point represents the shadow region of the TRC.

Experimental Verification of Gray Balance Control

As pointed out before, a complete gray balance look up table requires the adjustments at the gamut boundaries; i.e., for highlights and shadow regions of the TRCs. The control of the shadow region is achieved by adding to the CMY controller described above additional 100% patches of Cyan, Magenta and Yellow separations. The control of the highlight region is accomplished by simply positioning CMY patches more densely near the lower end of the TRC curve in order to assure a consistent extrapolation to the lowest input level, i.e., gray level 1 for most digital printers. The results of this kind of optimization are a test target design with a reduced number of patch set. For a 4x256 CMYK gray balanced TRC LUT, we required only 22 patches. Table 2 illustrates the input values of the target and the corresponding L*a*b* values. 22 patches were distributed across the neutral axis (CMY neutral and k patches. Additional knots, i.e., to find the threshold highlights, are obtained by extrapolation of three knots in the low digital input region. Then, the entire trc curve (0-255 values) is constructed by using a TRC smoothing algorithm described above. Extensive experimental and simulation results, were performed under a wide variety of conditions, which demonstrated that this methodology produces GB TRCs that enable printers to operate with $\Delta E < 3$ peak to peak (95%) between multiple calibrations.

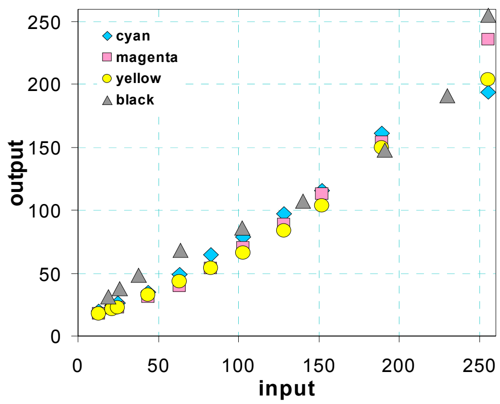

Figure 6. Gray Balance TRC at control nodes (experimental plot). Display of the 11 CMY knots and 8 measured K knots. An additional black knot, with input at 255, is predetermined to be output 255 (solid black).

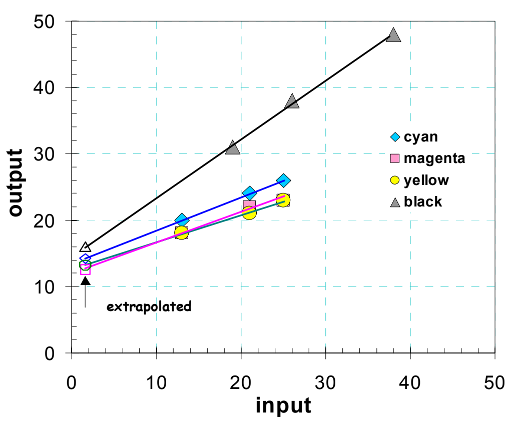

Figure 7. Determination of the threshold highlight by extrapolation of three low input knots.

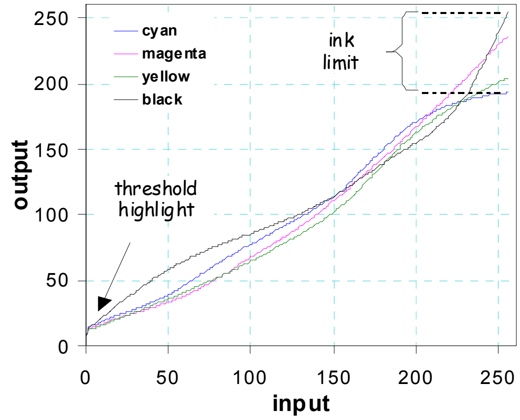

Figure 8. Final GB TRCs obtained using the procedure described in this paper

Table 2: Experimental Verification of the Gray Balance Procedure

Gbcalib patch set				
	Relative to Paper			AC input
Color	L*	a*	b*	
white	100	0.0	0.0	0
cmy (neutral)	95.3	-1.0	-0.7	5
	91.5	-0.9	-0.7	8
	90.2	-2.0	-1.5	10
	83.2	-0.8	-0.3	17
	75.3	-0.2	-2.0	25
	66.9	-1.2	-3.7	32
	59.2	-0.4	-1.2	40
	48.4	0.3	-2.5	50
	38.5	2.9	-2.4	60
	23.2	1.7	-2.6	74
cyan	47.4	-26.5	-62.1	100
magenta	43.7	81.0	-0.4	100
yellow	93.6	-8.8	108.2	100
black	16.1	1.7	4.5	90
	22.7	1.5	4.2	75
	41.6	1.1	3.3	55
	57.6	0.4	2.0	40
	71.5	0.2	0.8	25
	82.9	0.1	-0.1	15
	91.3	0.2	-0.2	10
	96.1	0.2	-0.4	7.5

Table 3: Calibration results table. Here AC0 corresponds to the initial calibration, and AC1, AC2 and AC3 to subsequent calibrations after disturbances AD1, AD2, and AD3. These results indicate that the GB calibrations are within the random noise of the printer IOT, which dominates the color variability of the patches.

Summary	dcg paper					
	20%			60%		
	DE95	DEmax	DEmean	DE95	DEmax	DEmean
AC0-AC1	2.26	3.28	1.00	3.86	7.56	1.61
AC0-AC2	1.39	2.38	0.65	2.82	5.43	1.24
AC0-AC3	2.01	3.01	0.86	3.06	5.51	1.33
Overall AC0-Acs	**2.03**	3.28	0.84	**3.33**	7.56	1.39
AC0-AD1	1.84	2.78	0.74	3.02	5.85	1.32
AC0-AD2	1.90	3.61	0.89	3.55	6.73	1.54
AC0-AD3	1.71	2.77	0.77	3.34	5.95	1.36
Overall AC0-Ads	**1.82**	3.61	0.80	**3.32**	6.73	1.41

Table 4: Summarizes the results of 3 different calibration algorithms used in commercially available digital front ends and for the algorithm presented in this paper. The control based algorithm was executed with inline spectrophotometer. To test the performance of these calibrations, we printed GAFT (SWOP) images and measured the K and CMY patches with AC inputs depicted in column 1 of Table 3 using a X-Rite 938 spectrophotometer. These results demonstrate that the GB calibration algorithm perform as good as these standard offline DFE calibrations.

Patches	Delta peak to peak (95%)				Control based algorithm performance differential			
	Alg1	Alg2	Alg3	Control based alg	Mn	Alg1	Alg2	Alg3
25K	1.67	1.57	3.18	1.61	1.57	-0.07	0.04	-1.58
50K	3.65	2.1	4.41	3.16	2.1	-0.49	1.06	-1.24
75K	5.22	3.76	1.92	1.92	1.92	-3.3	-1.84	0
25C, 16M, 16Y	6.38	3.66	2.34	3.22	1.72	-3.17	-0.44	0.88
50C, 39M, 39Y	10.06	1.72	3.35	3.38	1.72	-6.68	1.65	0.02
75C, 63M, 63Y,	10.41	3.25	3.82	4.34	3.25	-6.07	1.08	0.52

We also measured the performance of prints of CMYKRGB and neutral CMY patches with area coverage of 20% and 60% using the gray balance TRCs for variety of disturbances. Tables 3 and 4 summarize the performance of the control system.

Conclusions and Summary

We proposed a unique control based algorithm for gray balancing digital printers. It is iterative based, and uses minimal number of measurements to determine the gray balance inverse maps. Algorithm was verified extensively through computer simulation and experiments with offline and inline spectrophotometers.

References

1. P.K. Gurram, S.A. Dianat, L.K. Mestha, R. Bala, "Comparison of 1-D, 2-D and 3-D Printer Calibration Algorithms with Printer Drift", IS&T NIP21, 2005.
2. L.K. Mestha, Eric Jackson, Y.R. Wang, M.E. Banton, P.A. Crean, S.J. Harrington, E.J. Solcz, "Color adjustment apparatus and method", US Patent# 6,744,531, June 1st 2004
3. G. Sharma, "Digital Color Imaging Handbook", CRC Press, ISBN 0-8493-0900
4. K. Ogata, "Discrete-Time Control Systems", Prentice Hall 1987, ISBN 0-13-216102-8
5. L.K. Mestha, S. Dianat "TRC Smoothing algorithm to improve image contours in 1D color controls", US Patent Application, March 2005

Author Biographies

L.K. Mestha, a Principal Scientist at Xerox, received his PhD from the University of Bath, England in 1985 and his BE in 1982, from the University of Mysore, India, all in EE. He has worked on sensing and control of digital printing systems since 1994. He holds 40 US Patents and has a total of 100 publications including patents & patent filings. Prior to joining Xerox, Mestha was at the SSC Laboratory in Dallas. He is a Senior Member of IEEE, a member of IS&T and teaches at RIT as an Adjunct Professor.

R. Enrique Viturro, Ph.D. –Technion, Israel, is Research Staff Member of the Wilson Center for Research and Technology of the Xerox Corporation. Since joining Xerox in 1985, he has worked on research, development and implementation of novel technologies for digital printing systems. He has published over 60 technical papers and has over 25 US patents and patent applications in areas of color electrophotography and printing processes. He is a member of INCOSE, of the APS, and pass member of the Executive Committee of the NYSS-APS.

Y.R. Wang obtained his PhD in 1986 from Department of Physics, Purdue University. Since then, he has been doing research and development work at Xerox Wilson Center for Research & Technology in the area of solid state physics, process and color control and management, and MEMS device development. He has over 70 publications and over 10 patents.

Sohail A. Dianat received the B.S. degree from Arya-Mehr University, Tehran, Iran in 1973, and the M.S. and D.Sc. degrees from George Washington University in 1976 and 1981, respectively, all in electrical engineering. Professor Dianat has been with the Department of Electrical Engineering at RIT since 1981. Sohail is the author of numerous publications. He received the "best unclassified paper award" at the MILCOM '93. He is fellow member of SPIE and a member of IEEE.